Journal of Network Intelligence
Taiwan Ubiquitous Information
 ISSN 2414-8105 (Online)
Volume **7**, Number **3**, August **2022**

Research on Porosity Detection Method for Welding X-ray Images

Guo-Lin Xu*[1] and Qi Cheng[1]

School of Computer Science and Technology
Chongqing University of Posts and Telecommunications
Chongqing 400065, P.R.China
xuguolin0626@gmail.com and chengqi0113@gmail.com

Ling-Xiao Wei[2]

School of Computer Science and Technology
Chongqing University of Posts and Telecommunications
Chongqing 400065, P.R.China
weitou1113@gmail.com

Jian-Xun Mi[3]

School of Computer Science and Technology
Chongqing University of Posts and Telecommunications
Chongqing 400065, P.R.China
mijianxun@gmail.com

*Corresponding author: Guo-Lin Xu

Received April 2, 2022, revised May 11, 2022, accepted June 10, 2022.

Abstract. *Welding is one of the critical material processing technology in modern industrial production, the defect detection of which is a key part of the production process. Porosity is a defect that is easily produced during welding, and the presence of porosity can degrade the quality of the weld formed. This paper proposes a two-stage approach based on the Faster R-CNN algorithm for detecting porosity in X-ray images, i.e., locating the weld seam first and then detecting the porosity, and using FPN for feature fusion, which effectively solves the problem that it is difficult to detect porosity at different scales simultaneously, and also includes a sliding window cropping method and an image enhancement strategy to further improve the detection effect of porosity.*
Keywords: Welding Defects, Object Detection, Feature Fusion, Faster R-CNN

1. **Introduction.** Welding is widely used in the petrochemical, aerospace, and marine industries as one of the important material processing processes in modern industrial production. Welding defects reduce the quality of the welded workpiece, which directly affects the service life of the welded workpiece and is a dangerous hazard for serious safety accidents, such as the presence of defects in pressure pipelines, prone to leakage or even bursting [1]. Welding defects are usually divided into pores, cracks, incomplete fusion, incomplete penetration, slag inclusion, and other defects. Different welding defects have different effects on the structural strength, and overall performance of the welded parts, the presence of porosity defects could reduce the effective bearing cross-sectional area of the weld and stress concentration, jeopardizing the mechanical properties of the weld. Therefore, porosity is an important element of weld quality inspection. X-ray detection technology, ultrasonic testing technology, and metallographic microscope photography

detection technology are currently the most widely used non-destructive testing techniques for porosity defects [2]. X-ray detect detection is widely used in the detection of welding defects because of its intuitive imaging in digital images and the advantages of easy determining the size and internal location of defects. X-ray defect detection uses X-rays to penetrate the weld, and because of the difference in the ability of different densities of material to absorb X-rays, the difference in absorption can be distinguished from different densities of material, and the defects inside the weld will be reflected in the X-ray image, as shown in Figure 1. At this stage of industrial welding defect detection, most defects are identified by the inspector using the naked eye to examine the welding X-ray image. This method consumes a lot of human resources, has high detection costs, and detection speed is difficult to meet the growing demand for detection, necessitating the urgent development of an automatic detection method to achieve intelligent industrial upgrading.

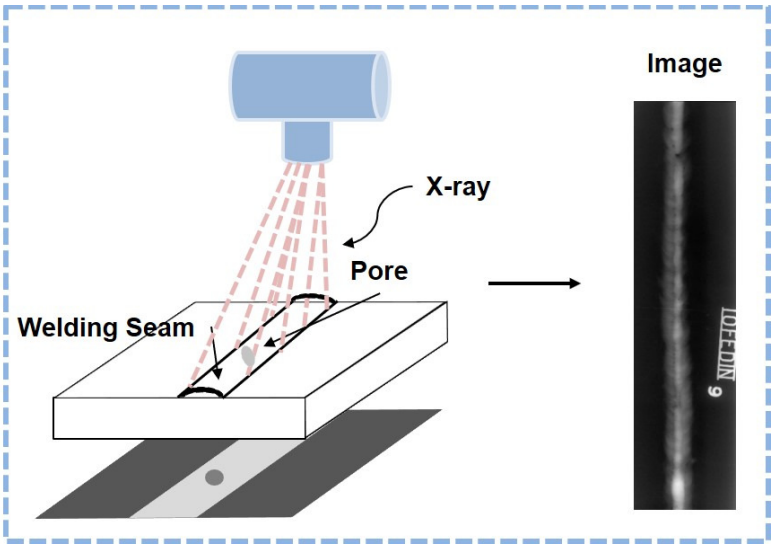

FIGURE 1. X-ray Defect Detection

With the development of image processing technology, the automated detection of welding defects based on welding X-ray images has received the attention of many scholars, and several existing studies have accumulated literature on the segmentation and classification of welding defects. Zhou et al. [3] proposed a method to construct an ideal weld background for image silhouette segmentation of suspicious defects, which identifies suspicious defects and does not qualitatively classify them. Chen et al. [4] proposed an unsupervised learning-based detection algorithm for constructing ideal weld backgrounds and test image subtraction to segment porosity defects, which has the advantage of detecting porosity defects without the need for manual marking. This method of constructing an ideal weld background for silhouetting necessitates a high-quality experimental image background, as well as a high degree of consistency in the image background. With the continuous upgrading of hardware platforms, some research workers have implemented the classification of defects inside the weld seam by using deep learning methods. Boaretto and Mezzadri Centeno [5] proposed a method based on Multilayer Perceptron and Back-Propagation Algorithm to classify defective and defect-free weld seams by considering segmented discontinuous regions in the seam as potential defects. Zhang et al. [6] proposed a multi-model integration framework for the classification of welding defects by combining the results of two models to determine the presence of a defect. For welding defect classification, Lei et al. [7] suggested an AlexNet-based multi-feature fusion technique.

The above work focuses on the segmentation and classification of welding defects. However, in practical industrial needs, not only is defect identification required, but also the determination of the specific location and size of defects in the X-ray image, as well as the number of defects in the category, such as porosity defects, where the size and number of porosity in the weld have varying degrees of impact on the quality of welded parts. Due to the complexity of the welding environment, the imaged welding X-ray images have unique characteristics: they are mostly large-size images with weak contrast and texture. As a result, the study object pores are small objects relative to the entire image, and the pores have variable scale features. In the face of these problems, in order to achieve the detection of porosity in X-ray images at different scales, this paper further investigates the object detection algorithms based on deep learning, which are currently divided into two main categories: one-stage algorithms based on regression and two-stage algorithms based on region proposals. One-stage algorithms are represented by the YOLO series of models, which is represented by end-to-end from the input image to direct output category and bounding box, and is characterized by fast computation but low detection accuracy. Typical representatives of two-stage algorithms include region-based convolutional neural network algorithm (R-CNN) [8], Fast R-CNN [9], Faster R-CNN, etc. For the R-CNN algorithm, each region proposals is fed separately into the convolutional neural network to extract features. To reduce the time consumed by the region proposals to extract features using the convolutional neural network, Fast R-CNN only performs feature extraction once for the whole image and uses the selective search method to produce region proposals, which still consumes a lot of time. 2016 Ren et al. [10] proposed the Faster R-CNN algorithm, which introduced the Region Proposal Network (RPN) to solve the above problem, where the first stage extracts feature from the image first, and then uses RPN to localize the target based on the feature map information to get the candidate regions. The second stage crops out the corresponding features of the region proposals located in the feature map and performs the final classification and regression bounding box by ROI Align of the same size, which is characterized by relatively slow speed but high detection accuracy and generally higher detection effect than the one-stage algorithm in the small object detection problem.

This paper proposes a two-stage method based on the Faster R-CNN algorithm for automatic porosity detection : first, weld seam localization, and then detection of the internal porosity of the weld seam. Through experimental analysis and comparisons, we verified the effectiveness of the algorithm on a publicly available dataset (GDXray). The main contributions of this paper are as follows: (1) A sliding-window cropping method is given to handle the problem of detecting small objects in large-size images by cropping the useless noise information in the image background. (2) To address the problem of porosity being easily missed in weak-contrast X-ray images, global histogram equalization is applied to enhance the images. (3) Considering that porosity is a multi-scale object and weld seams also exist in multiple forms, the feature pyramid network(FPN) is introduced to achieve multi-feature fusion detection to improve the detection effect. This paper consists of five parts, the first part is the introduction, the second part is the problem analysis, the third part introduces the theory and methodology, the fourth part is the experiment and discussion, and finally, the work done is summarized.

2. **Problem Analysis.** As shown in Figure 2, the welding X-ray images have the following characteristics based on the data presented: weak contrast, and differences in the background of each image, with a large amount of noise information in the background that might negatively affect the detection. In addition to the characteristics of the weld X-ray images, the scale variation of the porosity is also a challenge to be addressed in the

study. These problems present certain difficulties for the deep learning algorithms used in this study, which are analyzed in detail below.

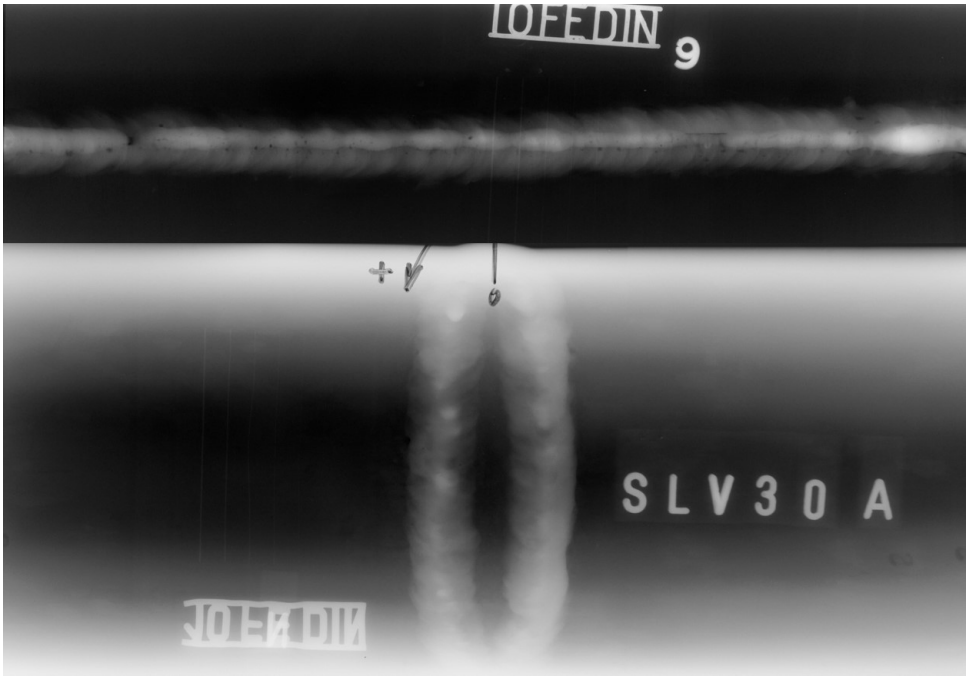

FIGURE 2. X-ray images

2.1. **Weak Contrast.** The low contrast images make the background of the x-ray images similar to that of the porosity during model training, resulting in poor feature response of the network to the porosity, making it difficult to extract effective features, resulting in missed porosity detection. Therefore, the quality of X-ray images needs to be improved.

2.2. **Large Size Images.** The GDXray dataset contains X-ray images mostly in the range of [4000,5000] pixels in length and [1000,2000] pixels in width. Due to the limitation of model input, the images cannot be directly used for model training and testing. According to statistical data, the smallest porosity is 12×16 pixels, and to ensure that small porosity can also be accurately detected, the X-ray images cannot be directly reduced and input to the model, otherwise the features of small porosity will be severely lost during the process of image downsampling and reduction, making it difficult for the network to extract effective features. Based on the aforementioned possible problems, a reasonable cropping of the image is an important precondition to achieving accurate detection of porosity.

2.3. **Multi-Scale Porosity.** Through the observation of the dataset, it is found that there are two shapes of porosity, circular and striped, along with multi-scale variations, and further, we made a pixel size histogram, as shown in Figure 3. According to the figure, it can be seen that more porosity has a size below 32×32 pixels, and there exists some porosity with a size more than 96× 96 pixels. As the number of network layers deepens, the semantic information of small porosity is lost in the deep feature extraction network, while large porosity can only be detected by extracting enough features in the deep network. The large differences in the shape and scale of porosity lead to the difficulty for the model to detect both small and large porosity, and it is necessary to implement multi-feature fusion in the porosity detection task in this paper.

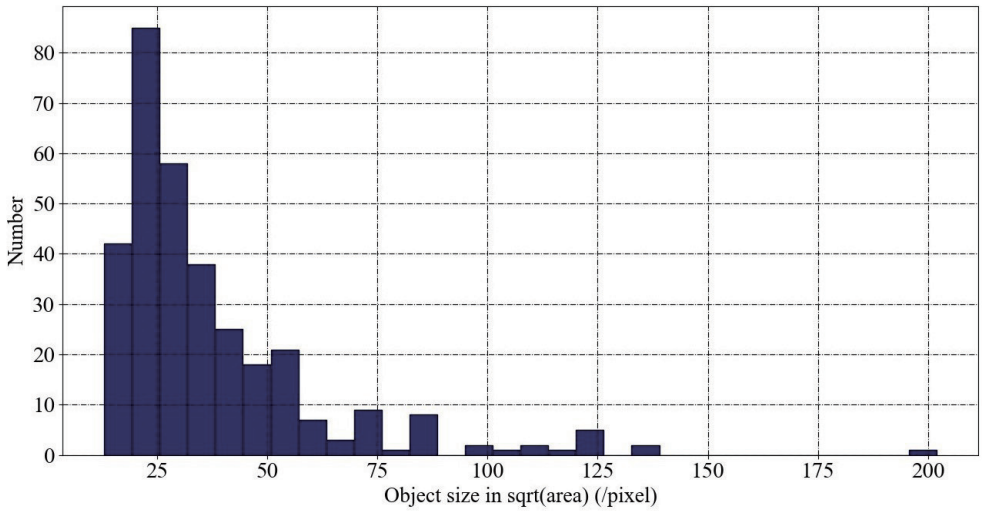

FIGURE 3. Histogram of Porosity Pixel Size

3. Theory And Methodology.

3.1. **Model Selection.** In this paper, we focus on the Faster R-CNN algorithm applied to weld seam and porosity detection in industrial welding X-ray images.

The Faster R-CNN algorithm consists primarily of extracting feature maps by feeding the entire image into the feature extraction network, directly generating region proposals by feeding the feature maps into the RPN, determining whether the anchors are positive or negative by softmax in the RPN, and then using the bounding box regression to fix anchors to get exact proposals, and the ROI Pooling layer collects the proposals and feature maps to calculate the proposal feature maps and input them to the second stage network for classification and bounding box regression again.

Figure 4 shows the basic network architecture of the Faster R-CNN algorithm. In subsequent studies, He et al. [11] proposed to change the ROI Pooling layer to the ROI Align layer, and Lin et al. [12] introduced the FPN into the feature extraction network, and these improvements further enhanced the detection performance of the Faster R-CNN algorithm.

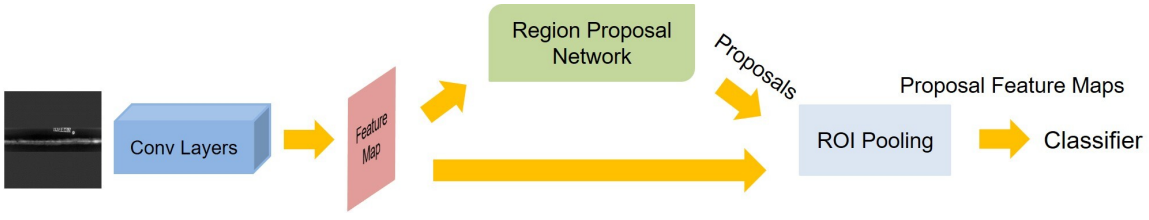

FIGURE 4. Faster R-CNN Network Architecture

3.2. **Transfer Learning.** The dataset used in this paper is small-scale data, and it is difficult to retrain the feature extraction network if random initialization of weights is used. To extract better features from X-ray images, a pre-trained feature extraction network is used as a feature extractor by combining the transfer learning. The X-ray images dataset is grayscale since the pre-trained model is based on the ImageNet [13] dataset. As a result, the feature extraction network needs to be globally fine-tuned during the model training.

3.3. **Sliding Window Cropping.** The work of cropping X-ray images can be divided into the following two steps: First, the weld seam is detected using the weld seam positioning algorithm, and after determining the specific location of the weld seam, the cropping width W is determined by the mode of the width of all weld seams. Lower-than-cut-width weld seams will be trimmed by maintaining a portion of the background, while higher-than-cut-width weld seams will be trimmed by the original width. Second, a sliding window is used to crop the weld seam obtained in the first step from left to right and from top to bottom. The window size is the cropping width W, and the sliding step size is W - m, where m is the maximum pore width, and the cropped adjacent sub-images will retain part of the overlapping area to ensure that the pore defects at the edges will not be destroyed by cropping. The final weld X-ray image with length and width dimensions of W. The X-ray image cropping process is shown in Figure 5.

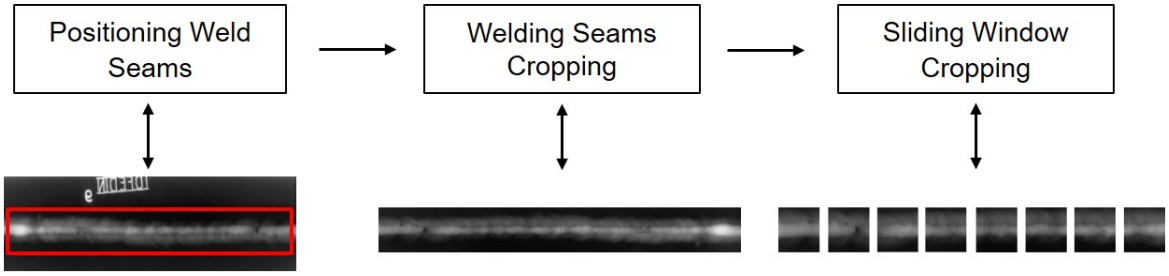

FIGURE 5. X-Ray Image Cropping

3.4. **Image Enhancement.** For the problem of low contrast, the commonly used grayscale transformation methods are logarithmic transformation, gamma transformation, histogram equalization, etc. Through several experiments and analyses, as shown in Figure 6, the cropped X-ray images are subjected to global histogram equalization, which effectively highlights porosity defects in low-contrast images and improves the network feature extraction effect Figure 6(b).

3.5. **Welding Detection.** Compared to the internal defects of the weld, the weld seam occupies a larger part of the whole X-ray image, is a large object that is easy to observe, and is rich in morphological features. Due to the large size of the X-ray image, the input size range of the Faster R-CNN algorithm is [600,1000], and to meet the input requirements, the image is scaled down to 600 pixels on the long side of the image, and then the short side is scaled equally and made up to 600 pixels to obtain an X-ray image with pixel size 600×600. Finally, the scaled-down image is input into the model for welding detection, as shown in Figure 7. Due to the large size and feature richness of the weld seam itself, the feature loss caused by scaling has little impact on the learning of the network. Further considering that the weld seam morphology is divided into the strip and circular arc, and there is scale variation in both morphologies, a Feature Pyramid Network (FPN) is introduced to improve the welding detection performance.

3.6. **Porosity Detection.** For porosity detection, ResNet [14] is chosen as the feature extraction network, and the concept of residual connection in ResNet can alleviate the problem of feature information loss in different network layers for the porosity of different scaling sizes. The ReLU activation function in the network will induce information loss as the number of network layers deepens [15], and the pooling layer and decreasing resolution of the feature map will also cause information loss. ResNet improves the degradation problem of deep neural networks so that large porosity can still be observed in the feature

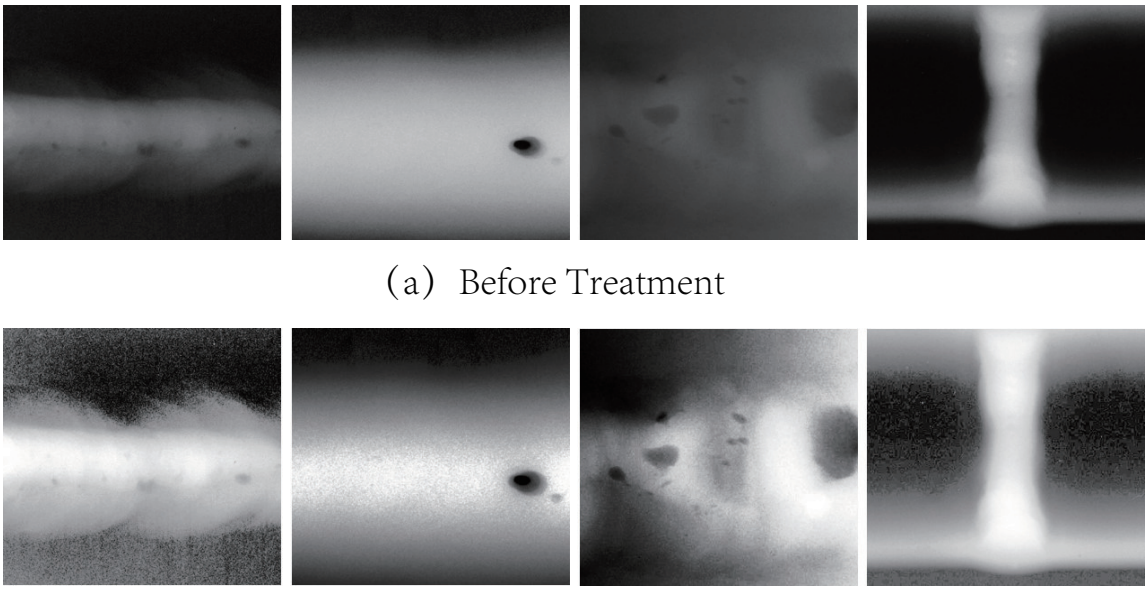

(a) Before Treatment

(b) After Treatment

FIGURE 6. Global Histogram Equalization of X-ray images

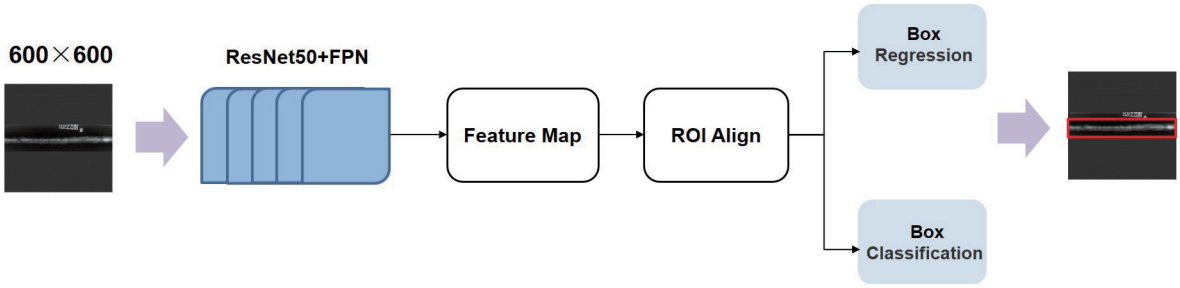

FIGURE 7. Welding Detection

maps output from deep networks. However, as shown in Figure 8, decreasing feature map resolution still inevitably results in the loss of small porosity features, which might lead to missed detection of small porosity. Therefore, it is difficult to meet the demand for porosity detection by relying only on the low-resolution feature maps of the deep network. To improve the recall rate of the network for multi-scale porosity, FPN is used in this paper to extract the features of porosity from the output feature maps of feature extraction networks at different levels. For small-size objects, the feature maps of the shallow network have a large resolution, where the features of small porosity are retained more relative to the feature maps of the deep network, but their semanticization is minimal, which is the opposite in the deep network. Therefore, it is impossible to achieve accurate detection of small porosity by relying only on the features of a certain level. The idea of FPN is to fuse deep feature maps and shallow feature maps to obtain feature maps containing advanced semantics and large resolution, which retains the feature information of small porosity in the shallow networks and improves the missed detection problem of small porosity. The deep network, on the other hand, can detect large porosity reliably, eliminating the influence of scale variation of porosity and enhancing the porosity recall rate.

The following is a summary of the work we've done to resolve the issues, as shown in Figure 9:

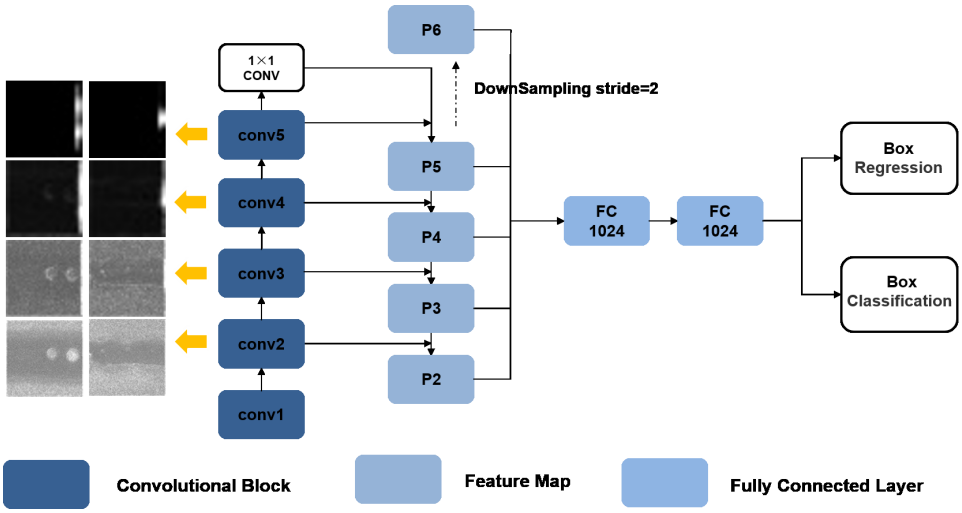

FIGURE 8. Feature Fusion-based Porosity Detection

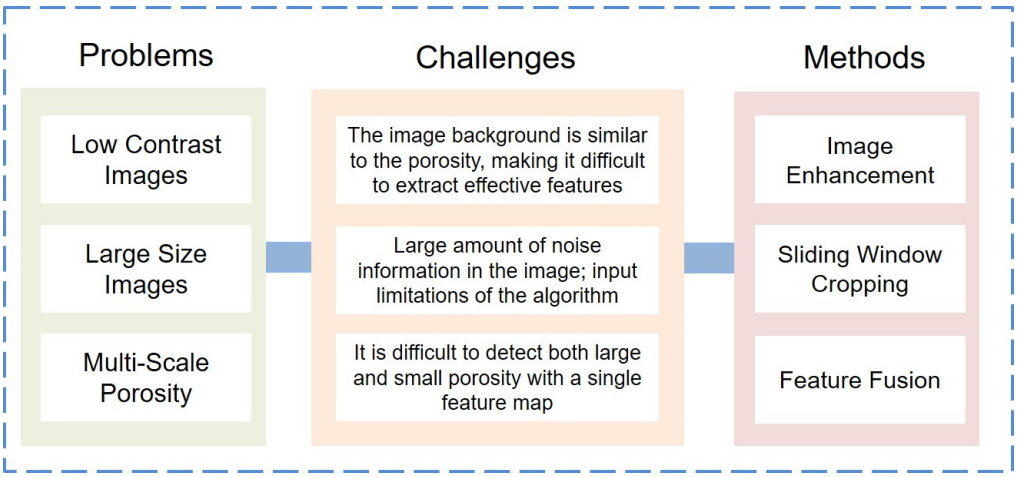

FIGURE 9. System Framework

4. Experiments and Discussion.

4.1. **Experimental Configuration.** GDXray [16] is a publicly available X-ray data set that includes data on X-ray welding images (Welds) collected by the BAM Federal Institute for Materials Research and Testing in Berlin, Germany. W0003 in the Welds dataset contains 68 X-ray images of welds. This paper is based on the W0003 data set, and with the help of welding experts, the welds and their internal defects were labeled and screened to obtain 36 X-ray images of the sheet with the presence of porosity. During the experiments, the dataset was divided into training and validation sets in the ratio of 2:1, and a tri-fold cross-validation was performed, and finally 176 images were obtained after cropping. For welding detection, combined with the previous analysis of the weld and considering the time factor, the one-stage algorithms YOLOv3 [17], YOLOv4 [18], YOLOv4-tiny [19], YOLOX-tiny [20], and the two-stage algorithms Faster R-CNN and Faster R-CNN+FPN for comparison experiments. For porosity detection, we select ResNet as the backbone network based on the Faster R-CNN algorithm and validate the effectiveness of three methods of image cropping, image enhancement, and

feature fusion by Ablation Experiments. The size of Anchors is set to [32,64,128,256,512], the aspect ratio is (1:2, 1:1, 2:1) and the data format is VOC2007.

4.2. **Evaluation Metrics and Specific Steps.** Recall and AP are two important metrics for evaluating object detection algorithms, as shown in Equation 1 and 2, where TP denotes true positive, FN denotes false negative, and $P(\widetilde{k})$ denotes the precision at different confidence levels.

$$\text{Recall } = \frac{TP}{TP + FN} \tag{1}$$

$$AP = \sum_{k=1}^{N} \max_{\tilde{k} \geq k} P(\tilde{k}) \Delta r(k) \tag{2}$$

Because the image is supplied to the model with a sliding window cropping, it is necessary to restore the image before computing Recall and AP during testing, as shown below: (1) Add the coordinates of the detected porosity to the coordinates of the upper left corner of the cropped image in the original image. (2) Non-Maximum Suppression (NMS) of the reduced porosity detection results is required because a portion of the overlapping area is retained during the sliding window cropping. (3) Calculate Recall and AP.

Table 1. Test Results of Different Weld Detection Algorithms

Model	Backbone	Evaluation Index	
		Recall(%)	AP (%)
Faster R-CNN	ResNet50	88.88	87.01
Faster R-CNN	ResNet50+FPN	96.30	93.76
YOLOv3	Darknet53	68.97	61.33
YOLOv4	CSPDarknet53	65.52	47.75
YOLOv4-tiny	CSPDarknet53-tiny	74.46	68.12
YOLOX-tiny	CSPDarknet53-tiny	94.83	88.20

4.3. **Test Results.** For welding detection, as shown in Table 1. Among them, YOLOv3 has a significantly better AP score with a similar recall rate compared to YOLOv4, which is due to the relatively large size of the YOLOv4 backbone network with a large number of parameters, which is prone to overfitting only for detecting weld seams as a class object, while on the lighter YOLOv4-tiny and YOLOX-tiny, both recall rate and AP score are improved. The difference between the two is that YOLOX is an Anchor-free algorithm, while YOLOv4 is an Anchor-based algorithm. Weld seam as a large scale target usually runs through the whole image, the Anchor-free algorithm is not limited to preset anchors and has a strong generalization ability and high accuracy of abnormal scale object detection, so the performance of YOLOX is substantially better than YOLOv4. But the two-stage algorithm Faster R-CNN+FPN has the best detection effect and outperforms the one-stage algorithm for the following reasons: compared to the one-stage algorithm, the RPN in the first stage of the two-stage algorithm has localized the weld seam and generated a large number of bounding boxes to ensure the recall rate. In the second stage, learning is performed based on the proposal feature maps output from ROI Align, then classification and regression bounding boxes are performed. The second regression of the bounding box is not limited to the preset anchors, and only the features corresponding to the location of each region proposals are used, resulting in high feature recognition and more accurate weld detection. The accurate detection of weld seam affects the subsequent defect detection task, so Faster R-CNN+FPN is the most applicable.

Table 2. Comparison Experiments Results of Different Cropping Methods

Model	Backbone	Cropping Method	Evaluation Index	
			Recall(%)	AP(%)
Faster R-CNN	ResNet50	Direct Scaling	26.53	5.38
		Segmented Cropping	49.38	10.93
		Sliding Window Cropping	74.92	61.38

After obtaining the coordinates of the weld seam by the welding detection algorithm, we need to extract the weld seam area to remove most of the noise information that does not need to be concerned in the study. There are two types of weld seams, strip and circular arc, and two types of weld seams exist for the strip type. In this paper, a long strip weld is defined as one with a length in the range of [4000,5000] and a width in the range of [300,1100], a short strip weld is defined as one with a length of [250,350] and a width of [600,700], and a circular arc type weld is defined as one with a length of [900,1200] and a width of [2000,2200]. Short strip welds can be directly input to the model for training and testing, while both long strip and circular arc welds require trimming, and the design of the trimming method determines the effectiveness of porosity detection.

In the experiments, a Faster R-CNN detection algorithm is chosen and ResNet50 is used as the backbone network. We compare three cropping methods: direct scaling, segmented cropping, and sliding window cropping. Direct scaling and segmented cropping extract the weld seam according to its specific coordinates in the original image while sliding window cropping takes the mode of the width of the weld seam as the cropping width, which is the first difference between the method and the first two methods. Since the final image pixel size obtained by sliding-window cropping is [600,600], the image size obtained by the first two methods is made the same as the latter to control the variables. For direct scaling, all welds are directly resized to [600,600] pixel size for training, and the detection results of porosity are shown in Table 2, which is consistent with the conclusions of the analysis above, where direct scaling leads to a decrease in image resolution, while the porosity itself is a small object and scaling leads to a loss of features of the porosity, thus making the detection worse. For segmented cropping, the specific operation is to crop long weld seams into 8 segments, circular weld seams into 3 segments, and short weld seams without cropping, and then resize all images to [600,600] pixel size for training after finally filtering out the data without pores, and the results show that segmented cropping is better than direct scaling for detecting pores. However, the difficulty with segmented cropping is that the porosity may be destroyed in the cropping process, and the data is reduced in the event of tiny batch data, and both of the above methods require resizing. For this kind of X-ray image with weak contrast and texture, resizing should be avoided. Because resizing causes the pore's morphology to stretch, resulting in the low accuracy of the model for porosity detection. Based on the above analysis, our sliding window cropping method crops the X-ray images from left to right and top to bottom through a fixed size window, and the final image size obtained without resizing protects the morphology of the pores, and the experimental result is shown in Table 2, the detection effect of pores is significantly improved.

For porosity detection, since most of pores are small in size, YOLO series algorithms are usually not suitable for small object detection tasks, and our preliminary experimental results also show that the YOLO series algorithm has a low recall rate for pores, and

TABLE 3. Ablation Experiments For Porosity Detection Performance Enhancement Strategy

Model	Backbone	Upgrade Strategy		Evaluation Index	
		Histogram Equalization	FPN	Recall(%)	AP(%)
Faster R-CNN	ResNet50			74.92	61.38
	ResNet50	✓		78.10	54.98
	ResNet34		✓	95.55	73.37
	ResNet50		✓	92.77	71.41
	ResNet101		✓	89.99	73.72
	ResNet34	✓	✓	96.85	70.08

there are more missed detections, which cannot meet the demand. As a result, the Faster R-CNN algorithm is used in the succeeding porosity detection research.

As shown in Table 3, ablation experiments were conducted on the feature fusion strategy choosing ResNet50 as the backbone network. The results show that the recall rate and AP score of the model for porosity are improved after introducing FPN. The results show that the recall rate and AP score of the model for porosity are improved after the introduction of FPN. The reason is that in the feature extraction stage, FPN upsamples the feature map of the deep network by ResNet50 and then fuses it with the feature map of the shallow network to get the final feature map, and the small porosity originally missed in the deep network are recalled, which makes the detection effect improved. Further, the ablation experiments are conducted for ResNet of different scales, and the results show that the small-scale network ResNet34 is more effective. Combined with the previous analysis of porosity detection at different scales, since the porosity themselves are not rich enough in features in the single-channel grayscale map, then the information loss will be further aggravated with the deepening of the network layers and the network is prone to overfitting. Meanwhile, due to the small dataset in this paper, it is difficult to fine-tune the large-scale pre-training weights effectively for a single-category object, which leads to a decrease in the detection effect.

To demonstrate the effect of global histogram equalization on image feature enhancement, comparison experiments were conducted based on the backbone network as ResNet50, as shown in Table 3, the recall rate was significantly increased with global histogram equalization, but the AP score was slightly decreased. The higher recall rate is owing to the image's higher contrast and the prominence of porosity in the background, making it easier for the network to extract porosity features. The decrease in AP score is because after global histogram equalization, the image feature expression is enhanced and the network recalls the labeled porosity along with some of the porosity unlabeled by the labelers, resulting in a lower AP score. In the field of industrial welding defect detection recall rate is a prerequisite for subsequent work, so improving recall rate is the primary research goal of this paper.

Finally, the detection performance of the Faster R-CNN algorithm for multi-scale porosity is significantly improved when the three approaches are combined.

5. **Summary.** A two-stage porosity detection method based on the Faster R-CNN algorithm is developed in this research to detect porosity at different scales in welding X-ray pictures, and the system's performance is proven on the public dataset GDXray. This paper's research findings are summarized as follows.

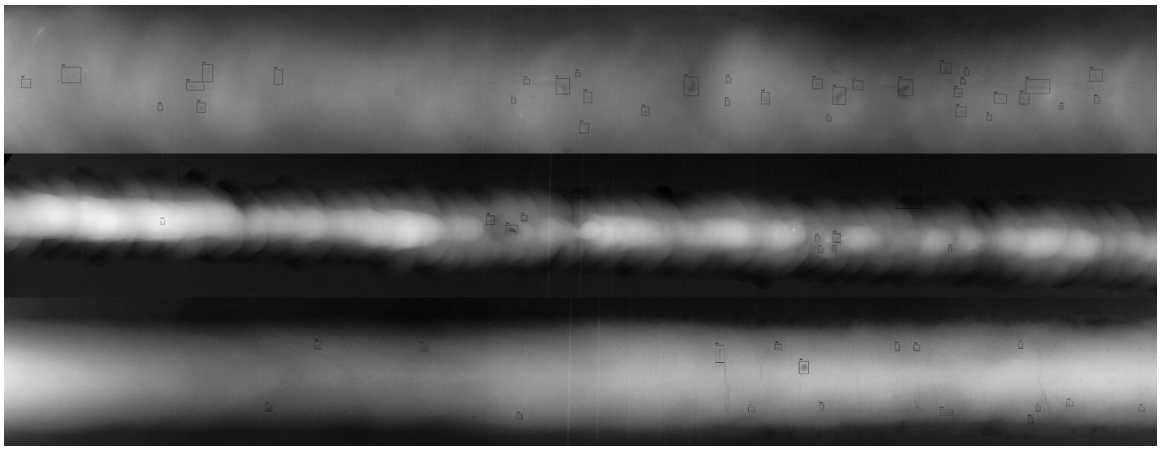

FIGURE 10. Porosity Detection Results

1. Rather than detecting porosity in X-ray images directly, this paper divides the porosity detection task into two stages, first detecting the weld seam and then detecting the porosity inside the weld seam, removing more redundant information from X-ray images and enhancing detection speed and effect.
2. A sliding-window cropping method is provided to crop large-size photographs into small-size images that may be directly input into the model, preserving the original image quality, preventing the destruction of porosity by cutting, and lowering the leakage detection of porosity by the model.
3. The global histogram equalization pre-processing method is employed to enhance the image feature expression and significantly improve the effect of porosity detection for welding X-ray images with low contrast.
4. To address the problem of multi-scale targets in porosity, this paper uses a feature fusion strategy and extends the feature extraction network in Faster R-CNN using FPN to improve the feature representation of porosity of various sizes, reducing porosity leakage detection and improving porosity localization accuracy.

We also discovered that the low contrast and blurred background of X-ray images affect defect data annotation, for example, when faced with multiple densely distributed defects, annotators use only one rectangular box to annotate; or when the size of defects in the image is small but the number of defects is large, there will be a small number of defect unlabeled. Low-quality labeling data has a significant impact on model detection, therefore future research will focus on a defect detection method based on semi-supervised learning.

Acknowledgment. This work was sponsored by Scientific and Technological Research Program of Chongqing Municipal Education Commission(Grant No. KJQN202100638).

REFERENCES

[1] G.-J. Mao, J.-H. Chai, Z.-J. Zhang, X.-L. Zhang, Z.-J. Lu, B.-K. Xue, J. Hu, and X.-J. Huang, "Weld detection of pipeline with medium based on x-ray computed radiographic technology," *Nondestructive Testing*, vol. 39, no. 10, pp. 37–41, 2017.

[2] P.-A. Duan, H. Zhang, G.-Q. You and P. Yan, "Research progress of welding porosity detection technology," *Hot Working Technology*, vol. 46, no. 5, pp. 19–24, 2017.

[3] H. Xiao, P.-F. Zhou, F. Wan and B. Ao, "Automatic detection and recognition of gas pores in dr images," *Nondestructive Testing*, vol. 39, no. 10, pp. 37–41, 2017.

[4] B.-Z. Chan, Z.-H. Fang, Y. Xia, L. Zhang, S.-R. Lan, and L.-S. Wang, "Automatic detection of blowholes defects in x-ray images of thick steel pipes," *Journal of Computer Applications*, vol. 37, no. 03, pp. 849–853, 2017.

[5] N. Boaretto and T. Mezzadri Centeno, "Automated detection of welding defects in pipelines from radiographic images dwdi," *Ndt & E International*, vol. 86, pp. 7–13, 2017.

[6] H.-D. Zhang, Z.-Z. Chen, C.-Q. Zhang, J.-T. Xi, and X.-Y. Le, "Weld defect detection based on deep learning method," *In 2019 IEEE 15th international conference on automation science and engineering (CASE)*, 2019, pp. 1574–1579.

[7] L. Yang, J.-F. Fan, B.-Y. Huo, and Y.-H. Liu, "Inspection of welding defect based on multi feature fusion and a convolutional network," *Journal of Nondestructive Evaluation*, vol. 40, no. 4, pp. 1–11, 2021.

[8] R. Girshick, J. Donahue, T. Darrell, and J. Malik, "Rich Feature Hierarchies for Accurate Object Detection and Semantic Segmentation," *2014 IEEE Conference on Computer Vision and Pattern Recognition*, 2014, pp. 580–587.

[9] R. Girshick, "Fast R-CNN," *2015 IEEE International Conference on Computer Vision*, 2015, pp. 1440–1448.

[10] S.-Q. Ren, K.-M. He, R. Girshick, and J. Sun, "Faster r-cnn: Towards real-time object detection with region proposal networks," *IEEE Trans Pattern Anal Mach Intell*, 2017, pp. 1137–1149.

[11] K.-M. He, G. Gkioxari, P. Dollár, and R. Girshick, "Mask R-CNN," *2017 IEEE International Conference on Computer Vision*, 2017, pp. 2980–2988.

[12] T.-Y. Lin, P. Dollar, R. Girshick, K.-M. He, B. Hariharan and S. Belongie, "Feature pyramid networks for object detection," *In Proceedings of the IEEE conference on computer vision and pattern recognition*, 2017, pp. 936–944.

[13] A. Krizhevsky, I. Sutskever, and G.-E. Hinton, "Imagenet classication with deep convolutional neural networks," *Communications of the ACM*, vol. 60, pp. 84–90, 2017.

[14] M. Sandler, A. Howard, M.-L. Zhu, A. Zhmoginov, and L.-C. Chen, "Mobilenetv2: Inverted residuals and linear bottlenecks," *In Proceedings of the IEEE conference on computer vision and pattern recognition*, 2018, pp. 4510–4520.

[15] K.-M. He, X.-Y. Zhang, S.-Q. Ren, and J. Sun, "Deep residual learning for image recognition," *In Proceedings of the IEEE conference on computer vision and pattern recognition*, 2016, pp. 770–778.

[16] D. Mery, V. Rio, U. Zscherpel, G. Mondragon, I. Lillo, I. Zuccar, H. Lobel, and M. Carrasco, "Gdxray: The database of x-ray images for nondestructive testing," *Journal of Nondestructive Evaluation*, vol. 34, no. 4, pp. 1–12, 2015.

[17] J. Redmon and A. Farhadi, "Yolov3: An incremental improvement," *arXiv:1804.02767 [cs.CV]*, 2018.

[18] A. Bochkovskiy, C.-Y. Wang, and H.-Y.-M. Liao, "Yolov4: Optimal speed and accuracy of object detection," *arXiv:2004.10934 [cs.CV]*, 2020.

[19] C.-Y. Wang, A. Bochkovskiy, and H.-Y.-M. Liao, "Scaled-yolov4: Scaling cross stage partial network," *In Proceedings of the IEEE conference on computer vision and pattern recognition*, 2021, pp. 13029–13038.

[20] Z. Ge, S.-T. Liu, F. Wang, Z.-M. Li, and J. Sun, "Yolox: Exceeding yolo series in 2021," *arXiv:2107.08430 [cs.CV]*, 2021.